Journal of Biomedical Informatics 55 (2015) 124–131

Contents lists available at ScienceDirect

Journal of Biomedical Informatics

journal homepage: www.elsevier.com/locate/yjbin

Development of a surgical navigation system based on augmented reality using an optical see-through head-mounted display

Xiaojun Chen [a,*], Lu Xu [a], Yiping Wang [a], Huixiang Wang [b], Fang Wang [b], Xiangsen Zeng [b], Qiugen Wang [b], Jan Egger [c]

[a] Institute of Biomedical Manufacturing and Life Quality Engineering, State Key Laboratory of Mechanical System and Vibration, School of Mechanical Engineering, Shanghai Jiao Tong University, Shanghai, China
[b] Shanghai First People's Hospital Affiliated to Shanghai Jiao Tong University School of Medicine, Shanghai, China
[c] Faculty of Computer Science and Biomedical Engineering, Institute for Computer Graphics and Vision, Graz University of Technology, Graz, Austria

ARTICLE INFO

Article history:
Received 24 August 2014
Revised 20 March 2015
Accepted 9 April 2015
Available online 13 April 2015

Keywords:
Surgical navigation
Augmented reality
Optical see-through HMD
Intra-operative motion tracking

ABSTRACT

The surgical navigation system has experienced tremendous development over the past decades for minimizing the risks and improving the precision of the surgery. Nowadays, Augmented Reality (AR)-based surgical navigation is a promising technology for clinical applications. In the AR system, virtual and actual reality are mixed, offering real-time, high-quality visualization of an extensive variety of information to the users (Moussa et al., 2012) [1]. For example, virtual anatomical structures such as soft tissues, blood vessels and nerves can be integrated with the real-world scenario in real time. In this study, an AR-based surgical navigation system (AR-SNS) is developed using an optical see-through HMD (head-mounted display), aiming at improving the safety and reliability of the surgery. With the use of this system, including the calibration of instruments, registration, and the calibration of HMD, the 3D virtual critical anatomical structures in the head-mounted display are aligned with the actual structures of patient in real-world scenario during the intra-operative motion tracking process. The accuracy verification experiment demonstrated that the mean distance and angular errors were respectively 0.809 ± 0.05 mm and 1.038° ± 0.05°, which was sufficient to meet the clinical requirements.

1. Introduction

During the past decades, computer-aided navigation system has experienced tremendous development for minimizing the risks and improving the precision of the surgery [2]. Nowadays, some commercially-available surgical navigation systems have already been tested and proved for clinical applications such as eNLight and NavSuite (Stryker Corporation, USA), Portable Nanostation (Praxim, France), and MATRIX POLAR (Scopis medical/XION, Germany). Meanwhile, many research groups also have presented their systems in the literature, for example, TUSS (Queen's University, Canada), VISIT (University of Vienna, Austria), IGOIS (Shanghai Jiao Tong University, China), etc. [3–7]. However, all of these systems use computer screen to render the navigation information such as the real-time position and orientation of the surgical instrument, and virtual path of preoperative surgical planning, so that the surgeons have to switch between the actual operation site and computer screen which is inconvenient and impact the continuity of surgery.

In recent years, due to the great development of Augmented Reality (AR) technology, more and more wearable AR devices have appeared like Google Glass, Skully AR-1 (An AR motorcycle helmet) [8], and etc. AR is an integrated technique of image processing, and in AR system, real objects and virtual (computer-generated) objects are combined in a real environment. Furthermore, real and virtual objects are aligned with each other, and run interactively in real time [1,9,10]. Due to the advantages of AR visualization, developing a surgical navigation system based on AR is a significant challenge for the next generation. For example, after the registration of the preoperative CT in relation to the intra-operative realistic scene, surgeons can superimpose the virtual CT data onto the patient's anatomy [11]. In 2010, Liao et al. [12,13] developed a 3-D augmented reality navigation system for MRI-guided surgery by using auto-stereoscopic images, and the system creates a 3D image, fixed in space, which is independent of viewer pose. In addition, Navab et al. [14] from Technical University of Munich have demonstrated a very practical

* Corresponding author at: Room 805, School of Mechanical Engineering, Shanghai Jiao Tong University, Dongchuan Road 800, Minhang District, Shanghai 200240, China. Tel.: +86 13472889728, +86 21 34204851; fax: +86 21 34206847.
E-mail address: xiaojunchen@163.com (X. Chen).

http://dx.doi.org/10.1016/j.jbi.2015.04.003
1532-0464/

application of AR. They developed an X-ray C-arm system equipped with a video camera, so that a fused image that combines a direct video view of a patient's elbow with the registered X-ray image of the humerus, radius, and ulna bones was produced.

This study presents an AR-based surgical navigation system (AR-SNS) using an optical see-through HMD (head-mounted display), which encompasses the preoperative surgical planning, registration, and intraoperative tracking. With the aid of AR-SNS, the surgeon wearing the HMD can obtain a fused image that virtual anatomical structures such as soft tissues, blood vessels and nerves integrated with the intra-operative real-world scenario, so that the safety and reliability of the surgery can be improved.

2. Materials and methods

2.1. The hardware architecture of AR-SNS

The AR-SNS is constructed based on a high-performance graphical workstation (HP), a 2D LCD monitor (G2200W, BenQ), an optical tracking device (Polaris Vicra, NDI Inc., Canada) and an optical see-through HMD (nVisor ST60, NVIS, United States) (Shown in Fig. 1). The workstation is equipped with a 4 GB memory card, a core i7 CPU and an nVIDIA Quadro FX4800 graphic card, running on the windows 7 operating system. As for HMD, it uses high-resolution microdisplays featuring 1280×1024 24-bit color pixels per eye, for vivid visual rendering and integration with reality.

2.2. The software framework of AR-SNS

The AR-SNS is developed under the platform of the Integrated Development Environment (IDE) of VS2008. All of the functions are programmed in Microsoft Visual C++ and some famous toolkits are also involved, such as the Visualization Toolkit (VTK, an open source, freely available software system for 3D computer graphics, image processing, and visualization etc., http://www.vtk.org/), CTK, ITK, IGSTK and QT, and then integrated into the AR-SNS.

Fig. 2 shows the framework of AR-SNS, and is described as follows: on the basis of the preoperative CT data of a patient, image segmentation is conducted, so that 3D models including hard and soft tissues, especially critical anatomical structures such as blood vessels and nerves can be reconstructed. After 3D reconstruction, preoperative planning is implemented so that an optimized osteotomy trajectory can be obtained. Then, with the support of the optical tracking device, the calibration of the surgical instruments is performed, and the point-to-point registration [15–17] and surface matching [18,19] methods are used to determine the spatial relationship between virtual coordinate system (VCS, refers to the computer screen coordinate system) and real coordinate system (RCS, refers to the patient coordinate system) [2]. In addition, an optical see-through head-mounted display is adopted so that an immersive augmented reality environment can be obtained and the virtual tissue can be integrated with the direct view. Finally, after calibration of the patient's position in relation to the HMD, the position and orientation of the virtual model will change with corresponds to the movement of HMD and patient, and match the real anatomical structures during intra-operative navigation process, so that the preoperative plan rendered in HMD can be transferred to the real operation site.

2.3. 3D-reconstruction and preoperative surgical planning

Based on the original CT data, the segmentation of the hard tissue is conducted by using a threshold and region growing combined method, and for the soft tissue in each image, semi-automatic region growing method is adopted, and if it is over-segmented or under-segmented, manual modification is also used. Then, 3D surface models can be reconstructed through the marching cubes algorithm [20]. Fig. 3 shows a 3D pelvis model and a bladder imported into AR-SNS after the 3D-reconstruction. All of the work including the image segmentation and 3D modeling is realized.

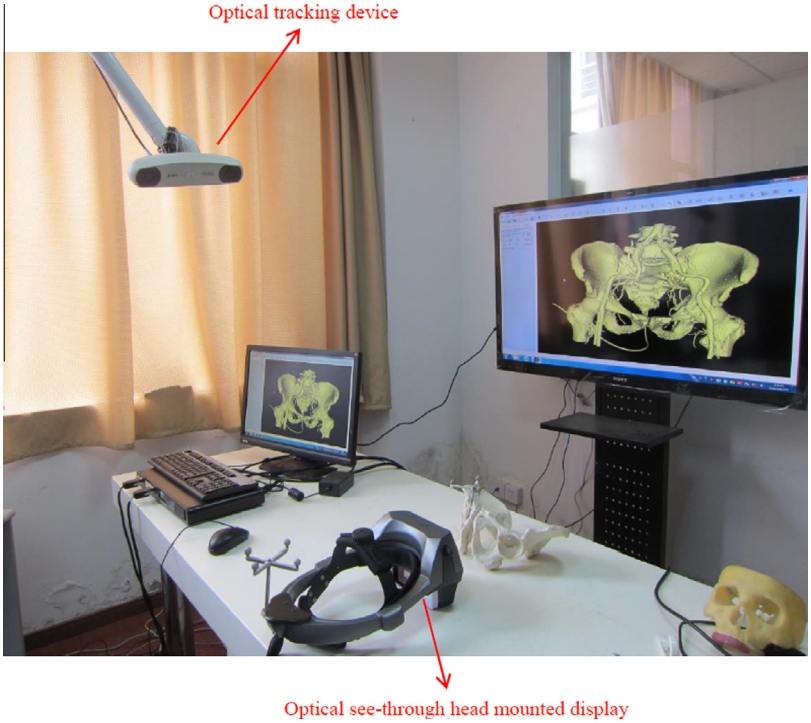

Fig. 1. The hardware of AR-SNS.

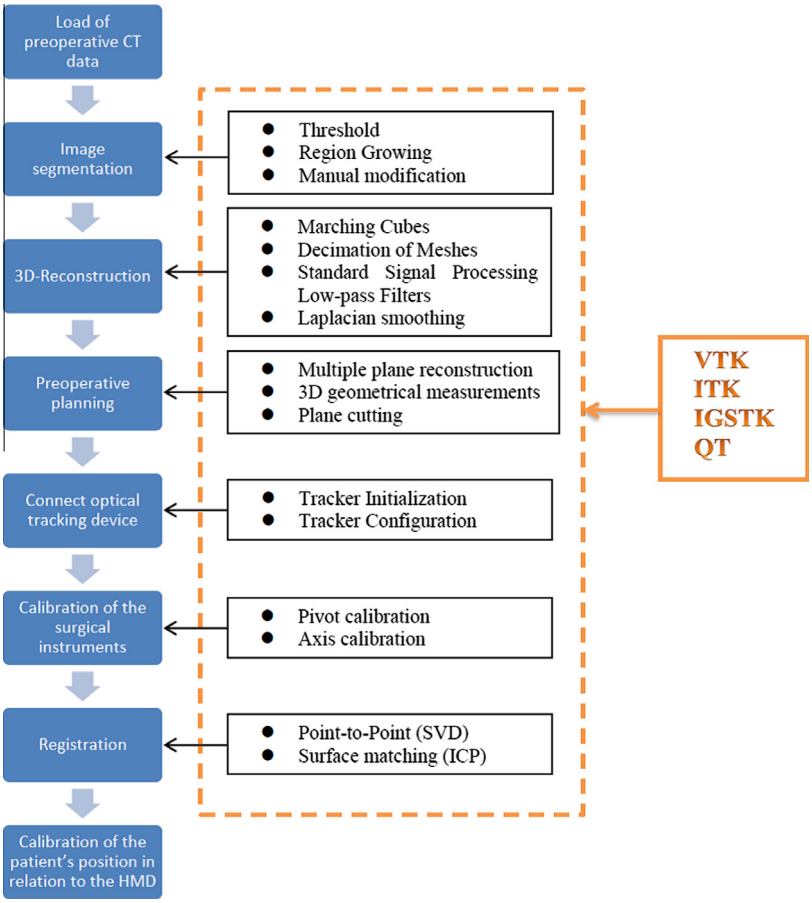

Fig. 2. The framework of AR-SNS.

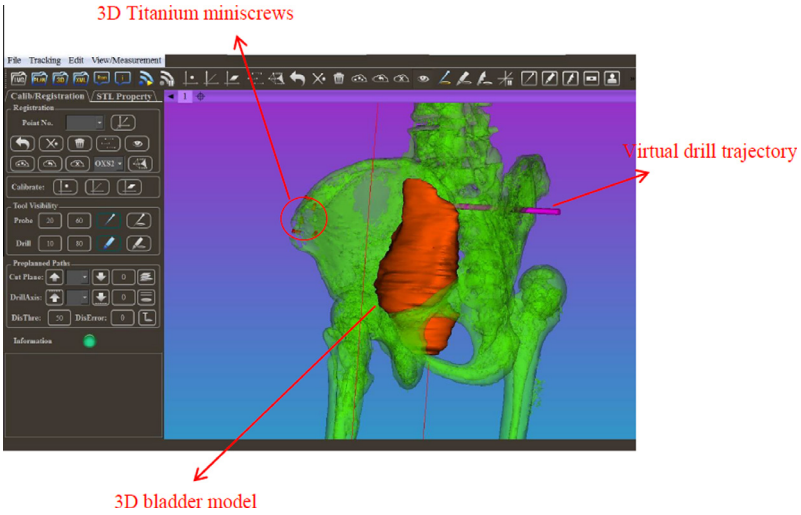

Fig. 3. A 3D pelvis model and a bladder imported into the AR-SNS.

On the basis of these CT images and the 3D model, the procedure of preoperative planning can be implemented and is describe as follows: percutaneous implantation of sacroiliac joint screw is a very common surgery in orthopedics. And, in order to avoid injuring the important anatomical structures like soft tissues, blood vessels and nerves, a virtual path for the surgical drill should be created and will be rendered on all of the 2D/3D views. An example for a preoperative surgical planning is shown in Fig. 4, so that the precision, safety and reliability of the implant surgery can be enhanced.

2.4. Registration

Since the Polaris Vicra optical tracking device only localizes the reference frame with mounted sphere-shaped retro-reflective markers, determining the spatial relationship between the surgical

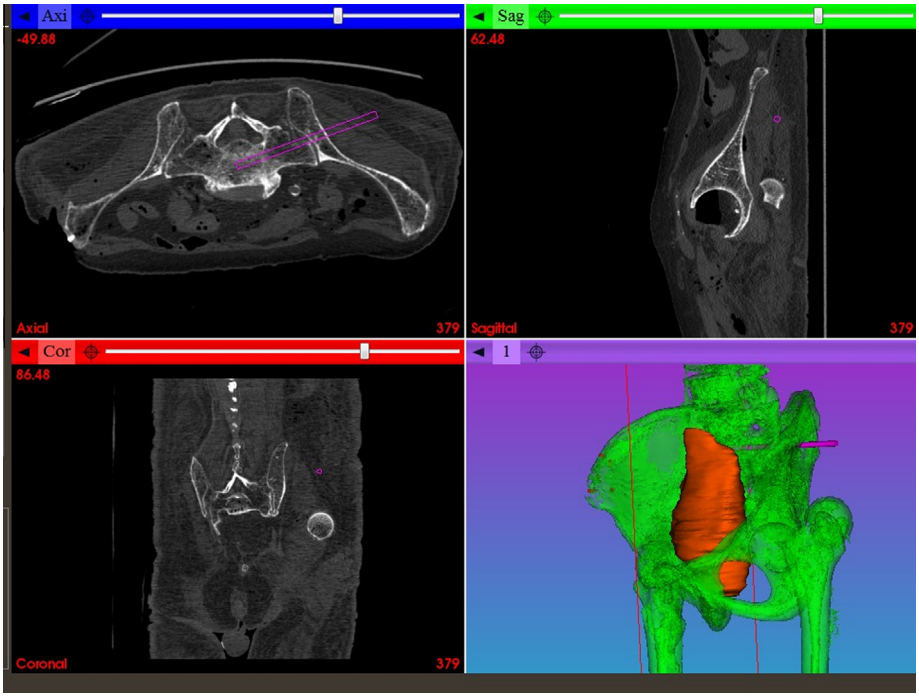

Fig. 4. A virtual path for the surgical drill rendering on all of the 2D/3D views.

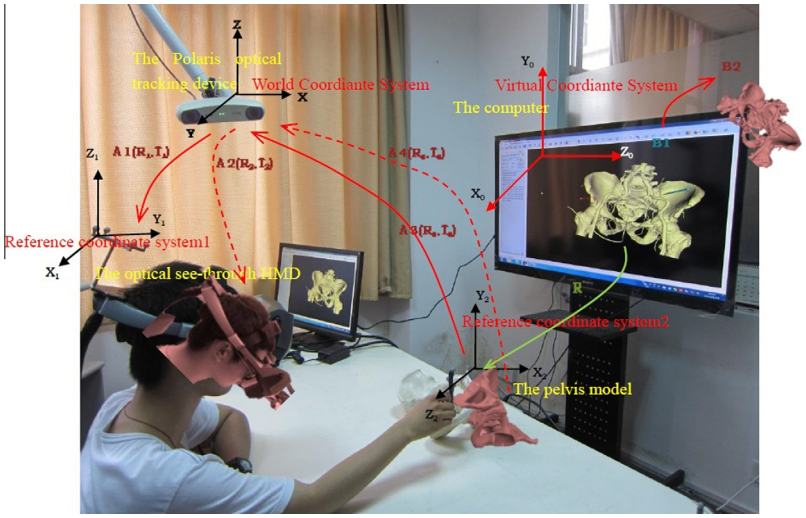

Fig. 5. The establishment of coordinate systems in AR-SNS.

instrument and the mounted reference frame (this procedure is also named as 'calibration') needs to be done first, so that the movements of the reference frame can represent those of the surgical instrument [21]. In AR-SNS, the pivot calibration approach is adopted and the Image-Guided Surgery Toolkit (IGSTK, an open-source C++ software library) provides classes for performing it [22], detailed principle of this calibration, please refer to Ref. [21].

The procedure of registration is an essential component for all computer-aided navigation systems, which brings two coordinate systems into spatial alignment [23]. In this study, the coordinate systems in AR-SNS are established in Fig. 5, and the VCS must be registered (aligned) with the reference frame coordinate system2 (also referred to as the patient coordinate system). A variety of registration methods, including point-to-point, surface-based, and template-based, are proposed. Among them, our AR-SNS integrates the fiducial point registration and surface registration together so that the registration accuracy is higher than traditional methods. As for the detailed description of the involved algorithms during this procedure, please refer to Ref. [2].

2.5. Calibration of the patient's position in relation to the HMD

After registration, the preoperative images in HMD are aligned with the patient on the procedure table. Then, the calibration of HMD needs to be done. In the AR-SNS, the basic requirement is the calibration of the patient's position in relation to the HMD, which means the movement of the patient or the HMD will not affect the initial correspondence of VCS and RCS. The principle is described as follows: first of all, two reference frames are respectively mounted on the HMD and patient. Then, in order to obtain

the calibration matrix after the initial registration of the patient's position in relation to the image data set, we built the transformation relationship shown in Fig. 5. Suppose:

R is the initial transformation matrix of VCS to reference frame coordinate system2;
A_1 and A_2 are respectively the transformation matrix of reference frame coordinate system1 to the World Coordinate System before and after movement of the user head;
A_3 and A_4 are respectively the transformation matrix of reference frame coordinate system2 to the World Coordinate System before and after movement of the patient;
B_1 is the matrix of virtual model under the VCS before movement;
B_2 is the calibration transformation matrix of virtual model under the VCS;

Since the relative position of one point on the computer virtual image is fixed before and after movement, setting X as the coordinate of this point in computer virtual image coordinate system. Then, X_1 is the coordinate of X in VCS (also referred as the computer screen coordinate system) before movement and X_2 is the coordinate of X in VCS after movement. Eq. (1) and Eq. (2) demonstrate the transformational relation:

$$RB_1X = X_1 \tag{1}$$

$$RB_2X = X_2 \tag{2}$$

The purpose is to maintain the relative position of this point in patient coordinate system unchanged before and after movement, so setting X_3 as the coordinate of X in reference frame coordinate system2. Eqs. (3) and (4) show the transformational relation before and after movement:

$$(A_3)^{-1}A_1X_1 = X_3 \tag{3}$$

$$(A_4)^{-1}A_2X_2 = X_3 \tag{4}$$

Thus, based on Eqs. (1)–(4):

$$B_2 = [(A_4)^{-1}A_2R]^{-1}(A_3)^{-1}A_1RB_1 \tag{5}$$

In the polaris optical tracking system, seven elements representing the unit quaternion and the translation vector, are used to describe the transformation of a rigid body under world coordinate system. Therefore, A_1, A_2, A_3, and A_4 can be calculated on the basis of each rigid body's seven elements provided by the Polaris, and R can be calculated through the point-based registration and surface registration respectively under patient coordinate system and virtual coordinate system.

Since A_1, A_2, A_3, A_4, R, B_1 (which can be supposed as an identity matrix) are all known, the calibration transformation matrix B_2 can be calculated according to Eq. (5). As a result, the position and orientation of the virtual model will change with corresponds to the movement of HMD and patient, and match the real anatomical structures during intra-operative navigation procedure.

The setup of the AR-SNS and the actual view seen from the HMD is also illustrated in Fig. 6.

3. The accuracy verification of AR-based surgical navigation system

The basic aim of using a surgical navigation system is to improve the surgical precision and prevent the intra-operative possible human errors. Therefore, the accuracy verification experiment for the AR-based surgical navigation system has been conducted. Fig. 7 shows a verification block designed in this study, which includes three components: a metal base, an organic glass substrate and a 3D-printed cranio-maxillofacial model. The design and manufacturing of the verification block is described as follows:

Based on the original CT scanning data of a volunteer, the virtual cranio-maxillofacial model was 3D reconstructed and assembled with the virtual metal base model using the UG software. Then, according to these data, the real nylon cranio-maxillofacial model was 3D printed using the high precision (0.1 mm) thermoplastics laser-sintering system (EOSINT P 395, Germany). The metal base was manufactured using the advanced 5-axis machine tool (DMU60, Germany) with the overall precision of 0.01 mm, and there were 175 taper holes (Diameter: 5 mm) and 40 through holes (Diameter: 4.2 mm) on its surface for measuring the distance error and angular error respectively.

3.1. The scheme of precision verification experiment

The precision verification process includes all procedures during the AR-based navigation surgery, for instance, CT scanning, 3D reconstruction, calibration of surgical instruments, registration, calibration of head-mounted display, real-time motion tracking, etc. The details are described as follows:

1. Mounting the reference frame on the metal verification block so that it can be tracked by the NDI Polaris Vicra tracking device.
2. Calibrating the positioning probe ("Pivot Calibration" and "Axis Calibration") through the calibration tool. Then, 5 or 6 fiducial landmarks can be collected on the surface of metal base and registered with the matched points on the virtual 3D model.
3. On the basis of the point-based registration, the point cloud can be collected on the surface of 3D printing model to implement the surface-based registration so that the registration errors can be corrected.
4. Calibrating the optical see-through head-mounted display when the user is wearing it. As a result, the 3D models are aligned with the real objects in the HMD during the intra-operative motion tracking process (see Fig. 8).
5. Using the probe to pick 100 target points in different regions of the metal base surface successively, and recording the actual coordinate of each point P_i (P_{ix}, P_{iy}, P_{iz}). Then, the actual coordinate is calculated with the theoretical coordinate of each point P_i^* (P_{ix}^*, P_{iy}^*, P_{iz}^*) to obtain the distance error P_{ierr}

$$P_{ierr} = \sqrt{\left(P_{ix} - P_{ix}^*\right)^2 + \left(P_{iy} - P_{iy}^*\right)^2 + \left(P_{iz} - P_{iz}^*\right)^2}, \quad (i = 0, 1, 2, \ldots, 99) \tag{6}$$

6. Inserting the probe into the 30 axial holes, and recording the actual axial direction A_i (A_{ix}, A_{iy}, A_{iz}). Then, the actual axial direction is calculated with the theoretical axial direction A_i^* (A_{ix}^*, A_{iy}^*, A_{iz}^*) to obtain the angular error A_{ierr}

$$A_{ierr} = \cos^{-1}\left[\left(A_{ix}\cdot A_{ix}^* + A_{iy}\cdot A_{iy}^* + A_{iz}\cdot A_{iz}^*\right) \Big/ \left(\sqrt{A_{ix}^2 + A_{iy}^2 + A_{iz}^2} \times \sqrt{A_{ix}^{*2} + A_{iy}^{*2} + A_{iz}^{*2}}\right)\right], (i = 0, 1, 2, \ldots, 29) \tag{7}$$

3.2. The results of the accuracy verification experiment

Before the experiment, the all 175 fiducial landmarks and 40 axial holes on the metal verification block surface were, respectively, divided into different regions (see Fig. 7).

Then, after the optical see-through head-mounted display was calibrated, we measured 100 target points and 30 axial holes in different regions and calculated the distance and angular errors, the results are shown in Table 1. During the measuring experiment,

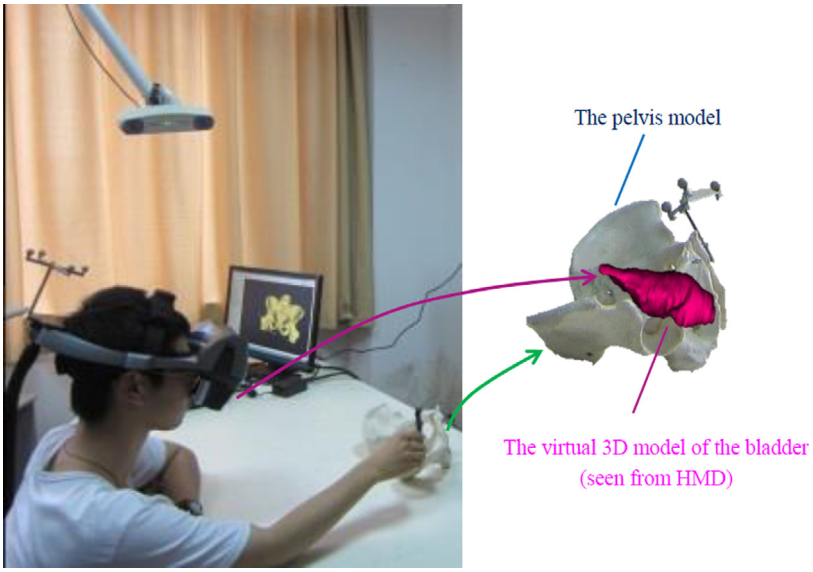

Fig. 6. Wearing HMD to conduct a phantom experiment.

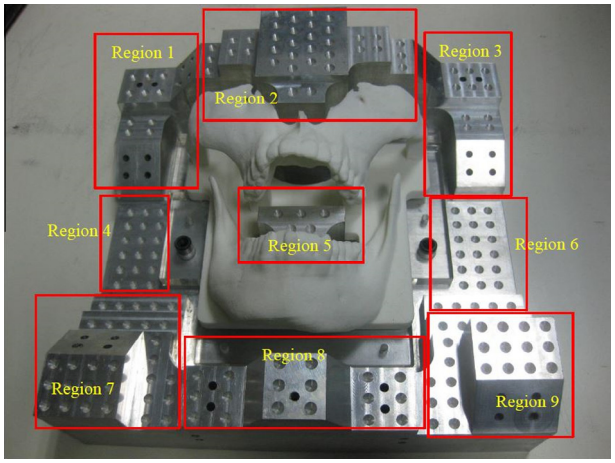

Fig. 7. The accuracy verification block.

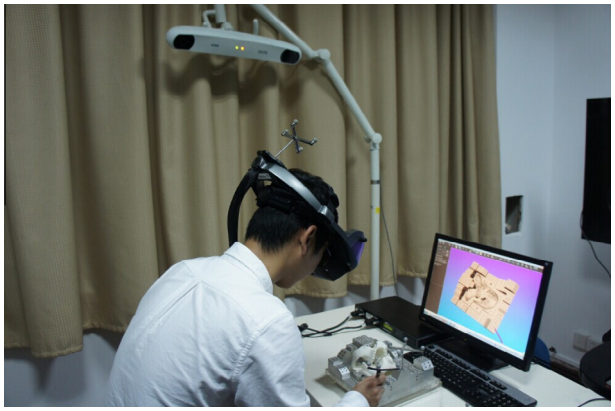

Fig. 8. The accuracy verification of AR-based surgical navigation system.

the maximum distance error of 100 target points was 1.125 mm, and the mean distance error was 0.809 ± 0.05 mm. Meanwhile, the maximum angular error of 30 axes was 1.308°, and the mean angular error was 1.038° ± 0.05°. According to the all results above, it demonstrated that the maximum distance and angular errors can be maintained less than 1.2 mm and 1.5°, and the error distribution

Table 1
The accuracy verification experiment.

Region	Distance error (mm)			Angular error (°)		
	Maximum	Minimum	Mean	Maximum	Minimum	Mean
1	1.056	0.542	0.855	1.126	0.958	1.026
2	0.916	0.608	0.768	1.218	1.012	1.092
3	1.118	0.660	0.868	1.135	0.972	1.018
4	1.125	0.562	0.823	1.072	0.967	0.989
5	1.066	0.596	0.718	0.998	0.916	0.954
6	0.970	0.515	0.776	1.116	0.962	1.008
7	1.108	0.624	0.812	1.308	0.856	1.113
8	1.079	0.658	0.874	1.158	0.922	1.032
9	1.048	0.592	0.791	1.250	0.908	1.106
Total	1.125	0.515	0.809	1.308	0.856	1.038

was also relatively average in different regions. Therefore, the accuracy of this AR-based surgical navigation system was sufficient to meet the clinical requirements.

4. Phantom experiment and cadaver experiment

A phantom experiment was first conducted. With the original CT data (0.625 mm slice thickness, 512 × 512 matrix), a 3D pelvis model was reconstructed through the threshold segmentation, and fabricated using 3D printing technology. Then, the critical anatomical structures (especially the soft tissues, blood vessels and nerves) can be segmented using the manual modification method. In this experiment, a 3D bladder and some blood vessels and nerves were reconstructed. After calibration and registration, the AR-based surgical navigation was realized. Seen through the HMD, the 3D virtual anatomical structures were aligned with the real plastic pelvis model in any time regardless of the movement of HMD and model (see Fig. 6).

Researchers have also conducted a cadaver experiment for percutaneous implantation of sacroiliac joint screw in an operating room. First of all, five titanium miniscrews were inserted into the pelvis before CT scanning for fiducial point registration. Then, based on the CT data, 3D-reconstruction and preoperative surgical planning were conducted, and the data were imported to AR-SNS. Fig. 3 shows the 3D- reconstruction, including a pelvis model, a bladder model and titanium miniscrews models. In addition, the optimization design of a virtual drill trajectory is the preoperative

planning result (see Fig. 4). Then, in order to show the position and orientation of the surgical drill model correctly, point calibration and axis calibration were carried out. After point-based and surface matching registration and calibration of the HMD, the 3D virtual bladder was aligned with the real cadaveric pelvis during the intra-operative process, and the 3D instrument model is displaying in HMD in real time, so that the operator can implant the sacroiliac joint screw into the pelvis along with the preoperative planned trajectory. (see Fig. 9)

5. Conclusion and discussion

The augmented reality technology has great potential to apply to the computer-aided surgical navigation system. Some examples of AR-based surgical applications have been presented in the literature, for example, a hybrid tracking method for surgical augmented reality (University of Tubingen, Germany), an integral videography system (University of Tokyo, Japan), an alternative biopsy guidance system (University of Pittsburgh, America), an X-ray C-arm system (Technical University of Munich, Germany), etc. In addition, the calibration of AR device is also introduced in some reports. For instance, Kellner (University of Kiel, Germany) et al. proposed a calibration approach with optical see-through head mounted displays to improve the average distance judgment of users in 2012, but, there is a significant underestimation of distances in the virtual environment [24]. Genc (Siemens Corporate Research Imaging and Visualization Department, America) et al. developed a method to calibrate stereoscopic optical see-through HMDs based on the 3D alignment of a target in the physical world with a virtual object in user's view [25]. However, the calibration algorithm was only validated on a video see-through system, and the researchers did not validate it for the optical see-through system. Gilson (Department of Physiology, United Kingdom) placed a camera inside an optical see-through HMD to take pictures simultaneously of tracked object and features in the HMD display for performing camera calibration [26]. In this study, a method for calibrating an optical see-through HMD is introduced and validated on an optical see-through system, and a surgical navigation system based on AR has been developed. Furthermore, unlike the video see-through HMD that the real-world view is captured with two miniature video cameras mounted on the head gear, the real world is seen through semi-transparent mirrors placed in front of the user's eyes with the optical see-through HMD. Therefore, the real- and virtual-world views are fused directly in the optical see-through HMD, and the impact on distortion of the field of view is slight.

Fig. 9. The panoramic view of the operating room for a cadaver experiment.

With the use of this system, including 3D-reconstruction, preoperative planning and registration, the 3D virtual critical anatomical structures in the optical see-through head-mounted display are aligned with the actual structures of patient in real-world scenario. During the surgery, the reference frames with mounted sphere-shaped retro-reflective markers are fixed on the patient and head-mounted display respectively so that their spatial positions can be localized in real time through the Polaris Vicra optical tracking device. Then, a method for calibrating the patient's position in relation to the HMD is proposed based on a series of spatial transformation. Therefore, the movements of HMD and patient will have little effect on the overlaid graphics after the calibration, and the position and orientation of the virtual model will match the real anatomical structures throughout the intra-operative navigation procedure. In addition, we can foresee calibrating in a real-world scenario during the registration procedure since the registration accuracy is much related to the HMD calibration effect. If the registration error value shown on the computer screen cannot meet the clinical requirements, it is required to repeat the registration procedure until it is satisfactory.

Therefore, some disadvantages of the traditional surgical navigation (For example, surgeon is no longer obliged to switch between the real operation scenario and computer screen) are overcome, and the safety, accuracy, and reliability of the surgery may be improved. Meanwhile, the results of the accuracy verification experiments show that it can be effective for the applications of minimally invasive surgery. The cadaver experiment validates the feasibility of AR-SNS. However, it is just a pilot study and still under development. Furthermore, some other experiments will be conducted to test the accuracy and efficiency of this system. The typical method is to measure the average distance deviations between the preoperative surgical planning trajectory and postoperative CT data. The researchers from Germany recently have compared the accuracy of a navigation system for oral implantology using either a head-mounted display or a monitor as a device for visualization. The results show that using of an HMD has no major disadvantages compared to the monitor setting [27].

Currently, there are also some commercially available computer-aided surgical systems. For example, the Da Vinci Xi® surgical robot (Intuitive Surgical, Inc., USA) enables surgeons to perform complex procedures through several interactive robotic arms [28]. In addition, the 3D image with crystal clear definition and natural color inside the patient's body can be seen with its 3D HD vision system. However, compared with our AR-SNS system, the mixed reality environment is not provided in it, which means the critical anatomical structures (blood vessels, nerves, etc.) cannot be seen until they are exposed. Furthermore, although the Da Vinci Xi® surgical system can translates the surgeon's hand, wrist and finger movements into precise, real-time movements of surgical instruments, the intra-operative navigation is not included and the surgeon still has to depend on his experience to operate. In our AR-based surgical navigation system, the surgical instruments can be tracked in real time and the virtual anatomical models can be simultaneously rendered in the HMD so that the pre-operative planning can be transformed to the actual surgical site correctly.

Meanwhile, there are still some technical challenges for further research and exploration. First, the measurement volume of "Polaris Vicra" optical tracking system in this experiment is restricted due to the dimension of this system is only 273 mm × 69 mm × 69 mm. As a result, sometimes the reference frame is out of tracking system and it is suggested to use another system named "Polaris Spectra", which has the larger dimension of 613 mm × 104 mm × 86 mm. In addition, the optical tracking result of reflective passive marker spheres attached on the reference frame will be impacted since the clinical environment is slightly wet. There is now a new kind of markers called "Radix

Lens", which has a smooth plastic surface that naturally sheds liquid and is easy to wipe clean to recover tracking. Moreover, since the immersion effect of virtual objects in the HMD is not so strong, a suitable focal length of HMD is required to be set for the practical surgical applications. Meanwhile, the real-time performance needs to be improved, since a little bit time latency occurs when the virtual critical anatomical structures are moving in the head-mounted display. Hence, we will not only improve the hardware but also the software algorithm to develop a delay free AR-based surgical navigation system, and some clinical trials will be conducted to validate the accuracy and reliability of AR-SNS. In addition, according to the feedback from the surgeons and human–machine interaction experts, we found that the bright colors of virtual anatomical models with the black background in the HMD had a more vivid mixed reality effect. Currently, our research group is also developing and integrating the hand gesture recognition function into AR-SNS with the Kinect (Microsoft Corporation, USA) device. Since the 3D position, orientation and full articulation of a human hand from markerless visual observations can be obtained by the Kinect sensor, the AR-SNS will provide more convenient and friendly user interactions for various surgeons [29].

Furthermore, due to the heavy weight of this optical see-through head-mounted display, surgeons will feel uncomfortable when wearing it to conduct the surgery for several hours. Recently, the Google Glass, a mini-computer with an 8-lb optical head-mounted display, has been widely used all over the world. So it has great potential to develop the AR-based surgical navigation system using Google Glass.

Currently, there is a well-known, free and open-sourced software package named 3D Slicer (http://www.slicer.org/) for visualization and medical image computing. It has been developed as a common research multi-platform with plenty of modules to support a wide variety of clinical applications such as visualization, segmentation, volume measurements, etc. Moreover, during the past several years, many research groups have developed loadable extension modules based on 3D Slicer, for example, DicomRtExport module enables basic DICOM RT studies to local storage [30] and iGyne module for MR-guided interstitial gynecologic brachytherapy [31]. Therefore, we also plan to integrate the AR-SNS into the 3D Slicer in the future so that it can be shared with the global research community.

Conflicts of interest

The authors declare that there are no conflicts of interest.

Acknowledgments

This study was supported by Natural Science Foundation of China (Grant No.: 81171429), Shanghai Pujiang Talent Program (Grant No.: 13PJD018) and Foundation of Science and Technology Commission of Shanghai Municipality (Grant No.: 14441901002). Dr. Jan Egger receives funding from the European grants ClinicIMPPACT (Grant No.: 610886) and GoSmart (Grant No.: 600641).

References

[1] G. Moussa, E. Radwan, K. Hussain, Augmented reality vehicle system: left-turn maneuver study, Transp. Res. Part C 21 (2012) 1–16.
[2] X.J. Chen, M. Ye, Y.P. Lin, Y.Q. Wu, C.T. Wang, Image guided oral implantology and its application in the placement of zygoma implants, Comput. Methods Programs Biomed. 93 (2009) 162–173.
[3] M.E. Kreissl, G. Heydecke, M.C. Metzger, R. Schoen, Zygoma implant-supported prosthetic rehabilitation after partial maxillectomy using surgical navigation: a clinical report, J. Prosthet. Dent. 97 (2007) 121–128.
[4] R. Ewers, K. Schicho, G. Undt, F. Wanschitz, M. Truppe, R. Seemann, et al., Basic research and 12 years of clinical experience in computer-assisted navigation technology: a review, Int. J. Oral Maxillofac. Surg. 34 (2005) 1–8.
[5] P. Grunert, K. Darabi, J. Espinosa, R. Filippi, Computer-aided navigation in neurosurgery, Neurosurg. Rev. 26 (2003) 73–99.
[6] U. Meyer, H.P. Wiesmann, C. Runte, T. Fillies, N. Meier, T. Lueth, et al., Evaluation of accuracy of insertion of dental implants and prosthetic treatment by computer-aided navigation in minipigs, Br. J. Oral Maxillofac. Surg. 41 (2003) 102–108.
[7] F. Watzinger, W. Birkfellner, F. Wanschitz, F. Ziya, A. Wagner, J. Kremser, et al., Placement of endosteal implants in the zygoma after maxillectomy: a cadaver study using surgical navigation, Plast. Reconstr. Surg. 107 (2001) 659–667.
[8] <http://www.skullsystems.com/#home>, (2014, June 10).
[9] R. Azuma, Y. Baillot, R. Behringer, S. Feiner, S. Julier, B. MacIntyre, Recent advances in augmented reality, IEEE Comput. Graphics Appl. 21 (2001) 34–47.
[10] M.D. Yang, C.F. Chao, K.S. Huang, L.Y. Lu, Y.P. Chen, Image-based 3D scene reconstruction and exploration in augmented reality, Automat. Constr. 33 (2013) 48–60.
[11] N. Navab, J. Traub, T. Sielhorst, M. Feuerstein, C. Bichlmeier, Action- and workflow-driven augmented reality for computer-aided medical procedures, IEEE Comput. Soc. 27 (2007) 10–14.
[12] H. Liao, T. Dohi, M. Iwahara, Improved viewing resolution of integral videography by use of rotated prism sheets, Opt. Express 15 (2007) 4814–4822.
[13] H. Liao, T. Inomata, I. Sakuma, T. Dohi, 3-D augmented reality for MRI-Guided surgery using integral videography autostereoscopic image overlay, IEEE Trans. Biomed. Eng. 57 (2010) 1476–1486.
[14] N. Navab, S.M. Heining, J. Traub, Camera augmented mobile C-arm (CAMC): calibration, accuracy study and clinical applications, IEEE Trans. Med. Imaging 29 (2010) 1412–1423.
[15] J.M. Fitzpatrick, J.B. West, C.R. Maurer, Predicting error in rigid-body point-based registration, IEEE Trans. Med. Imag. 17 (1998) 694–702.
[16] J.B. West, J.M. Fitzpatrick, S.A. Toms, C.R. Maurer, R.J. Maciunas, Fiducial point placement and the accuracy of point-based rigid body registration, Neurosurgery 48 (2001) 810–816.
[17] J. Claes, E. Koekelkoren, F.L. Wuyts, G.M.E. Claes, L. Van Den Hauwe, P.H. Van de Heyning, Accuracy of computer navigation in ear, nose, throat surgery – the influence of matching strategy, Otolaryngol. Head Neck Surg. 126 (2000) 1462–1466.
[18] K. Schicho, M. Figl, R. Seemann, M. Donat, M.L. Pretterklieber, W. Birkfellner, et al., Comparison of laser surface scanning and fiducial marker-based registration in frameless stereotaxy, Neurosurgery 106 (2007) 704–709.
[19] M. Caversaccio, D. Zulliger, R. Bachler, L.P. Nolte, R. Hausler, Practical aspects for optimal registration (matching) on the lateral skull base with an optical frameless computer-aided pointer system, Am. J. Otol. 21 (2000) 863–870.
[20] W.E. Lorensen, H.E. Cline, Marching cubes: a high resolution 3D surface construction algorithm, ACM Comput. Graph. 21 (1987) 38–44.
[21] X.J. Chen, Y.P. Lin, Y.Q. Wu, C.T. Wang, Real-time motion tracking in image-guided oral implantology, Int. J. Med. Robot. Comput. Assist Surg. 4 (2008) 339–347.
[22] K. Cleary, P. Cheng, A. Enquobahrie, Z. Yaniv, IGSTK: The Book, Signature Book Printing, Gaithersburg, Maryland, 2009, pp. 225–229.
[23] K. Cleary, T.M. Peters, Image-guided interventions: technology review and clinical applications, Annu. Rev. Biomed. Eng. 12 (2010) 119–142.
[24] F. Kellner, B. Bolte, G. Bruder, U. Rautenberg, F. Steinicke, M. Lappe, et al., Geometric calibration of head-mounted displays and its effects on distance estimation, IEEE Trans. Visual. Comput. Graph. 18 (2012) 589–596.
[25] Y. Genc, F. Sauer, F. Wenzel, M. Tuceryan, N. Navab, Optical see-through HMD calibration: a stereo method validated with a video see-through system, in: IEEE and ACM Int. Symposium on Augmented Reality, 2000, pp. 165–174.
[26] S.J. Gilson, A.W. Fitzgibbon, A. Glennerster, Spatial calibration of an optical see-through head mounted display, J. Neurosci. Methods 173 (2008) 140–146.
[27] B. Vigh, S. Muller, O. Ristow, H. Deppe, S. Holdstock, J.D. Hollander, et al., The use of a head-mounted display in oral implantology: a feasibility study, Int. J. CARS 9 (2014) 71–78.
[28] <https://www.davincisurgerycommunity.com/Home?tab1=HO>, 2015.
[29] X.Y. Zhang, Microsoft Kinect sensor and its effect, IEEE Multimedia 19 (2012) 4–10.
[30] <http://www.slicer.org/slicerWiki/index.php/Documentation/4.3/Modules/DicomRtExport>, (2013, November 5).
[31] X.J. Chen, J. Egger, Development of an open source software module for enhanced visualization during MR-guided interstitial gynecologic brachytherapy, SpringerPlus 3 (2014) 167–176.